Indian Journal of Chemistry
Vol. 64, January 2025, pp. 68-84
DOI: 10.56042/ijc.v64i1.14219

Quinazoline fused 1,2,4-triazoles: PIDA-mediated synthesis, characterization, anti-breast cancer agents, ABTS radical scavenging efficacy, molecular docking, and DFT studies

Parul Kaushik[a], Ravinder Kumar*[a], Gulshan Kumar[b], Rasdeep Kour[c], Sheikh Showkat Ahmad[c], Satwinderjeet Kaur[c] & Raj Kamal[d]

[a] Department of Chemistry, MMEC, Maharishi Markandeshwar (Deemed to be University), Mullana, Ambala 133 207, Haryana, India

[b] Department of Chemistry, Banasthali University, Banasthali Newai 304 022, Rajasthan, India

[c] Department of Botanical and Environmental Sciences, Guru Nanak Dev University, Amritsar 143 005, Punjab, India

[d] Department of Chemistry, Kurukshetra University, Kurukshetra 136 119, Haryana, India

E-mail: dr.ravinderkumar@mmumullana.org

Received 7 October 2024; accepted (revised) 27 November 2024

The present work demonstrates the PIDA-mediated mild synthesis of 3-aryl-5-phenyl-[1,2,4]triazolo[4,3-c]quinazolines **5a-n** through an intramolecular oxidative-cyclization of twelve electronically dissimilar and newly prepared (*E*)-4-(2-benzylidenehydrazineyl)-2-phenyl- quinazolines **4a-n** as key precursors. Structural confirmation of quinazoline-hydrazone and triazole has been established based on ^{1}H and ^{13}C NMR, IR, and HRMS data. Antiproliferative activity examination has led to the identification of 5-phenyl-3-(2,3,4-trimethoxyphenyl)-[1,2,4] triazolo[4,3-c]quinazoline **5g** and 3-(2,3-dichlorophenyl)-5-phenyl-[1,2,4]triazolo[4,3-c] quinazoline **5j**, as most active (less than and comparable to standard), which exhibit cytotoxicity with IC_{50} value of 1.14 mM and 1.39 mM, respectively against MCF-7 cell line. **5g** and **5j** also show significant potential against MDA-MB231 cell line with IC_{50} of 2.79 mM and 1.95 mM, respectively. Additionally, molecular modeling studies have been conducted to support the results and to study the binding interaction of the compound **5g** and **5j** with VEGFR-2 kinase enzyme (PDB ID:3U6J). Furthermore, systematic screening of **5a-n** for ABTS radical scavenging activity, displays that 3-(4-fluorophenyl)-5-phenyl-[1,2,4]triazolo[4,3-c]quinazoline **5h**, has the highest antioxidant efficacy with IC_{50}= 11.2 ± 0.14 µg/mL. The antioxidant efficacy of **5a-n** is also supported by DFT studies.

Keywords: [1,2,4]Triazolo[4,3-c]quinazolines, Hypervalent Iodine(III) Reagent, VEGFR-2 Inhibitors, Antiproliferative Activity, Antioxidant Activity

According to Cancer Statistics 2023[1], breast cancer accounts nearly 31% among all types of cancer in females (297,790 estimated cases).VEGFR-2 is highly up-regulated in tumors and play an imperative role in apoptosis. Therefore, it is essential to discover new therapeutic drug candidates with negligible side effects. Henceforth, blocking the activity of VEGFR-2 significantly disrupts the signaling pathway, thereby inducing angiogenesis and slowing down tumor growth. This mechanism provides us leading directional approach to discover cancer therapy. The requirement for new VEGFR-2 inhibitors rises due to the challenge posed by the development of resistance in cancer cells to existing chemotherapeutics.

Literature survey demonstrates that, especially nitrogen-heterocycles[2,3], unceasingly growing as excellent anticancer agents. In this context, quinazoline as the leading nitrogen heterocyclic scaffold recently highlighted as a highly effective chemotherapeutic agent[4, 5] with worldwide recognised biomedicinal activities such as antiplasmodial[6], antibacterial[7], anti-nematicidal[8], anticancer[9,10], anti-angiogenic[11], anti-alzheimer[12], anti-inflammatory[13], anti-tubercular[14], and imagining of atherosclerotic plaques[15], *etc.* that have been the subject of much research. Furthermore, quinazolines pharmacophore present as the fundamental skeleton of FDA-approved drugs[9,16,17] that includes anticancer: gefitinib, vandetanib and erlotinib; anti-malarial: febrifugine; anti-hypertensive: prazosin chlorhydate; and anti-inflammatory: proquazone (Fig. 1). This broad pharmacological potential produced by the quinazoline scaffolds has inspired organic chemist to advance their work in this field.

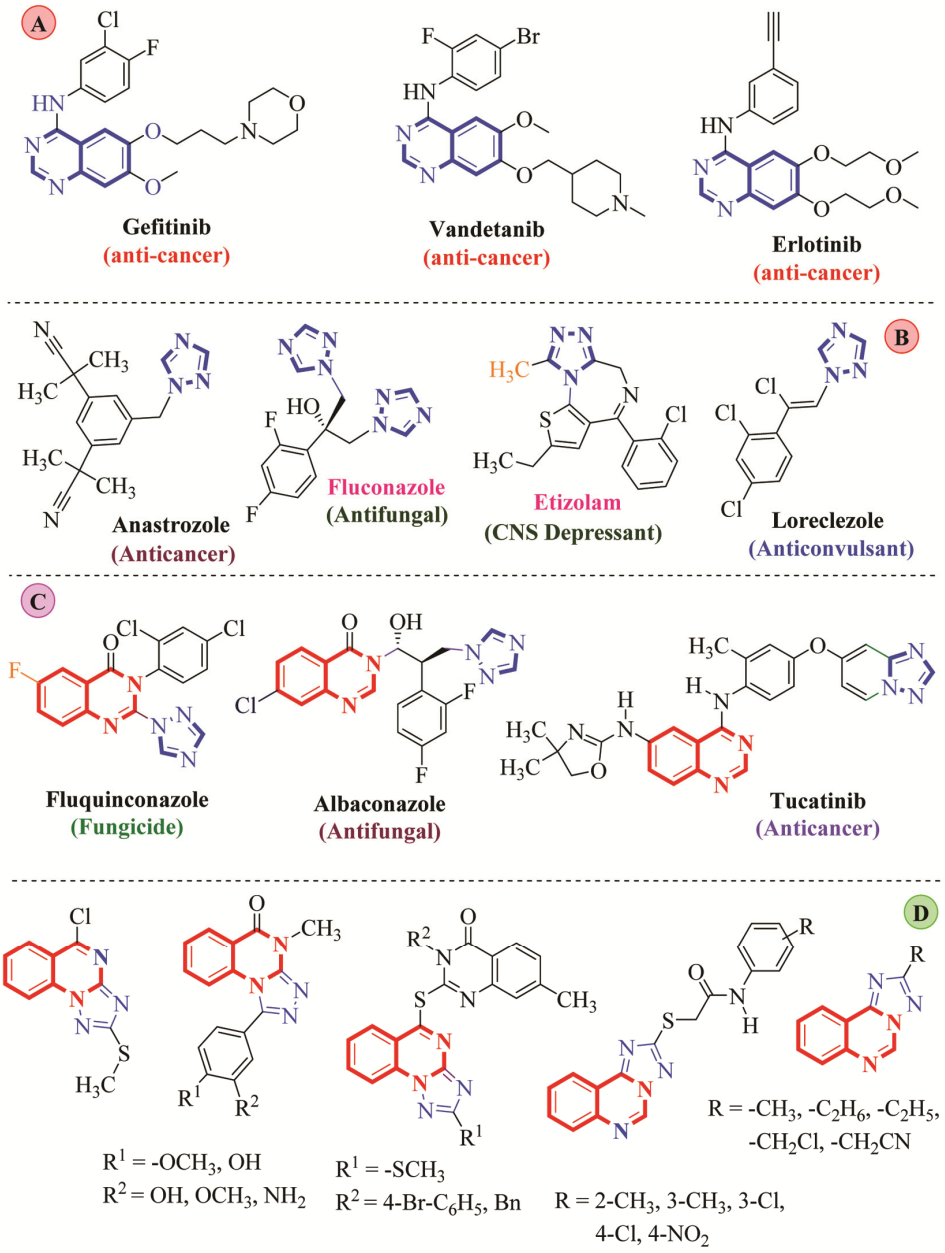

Fig. 1 — Selected quinazoline **(A)**, 1,2,4-triazole **(B)**, quinazoline linked 1,2,4-triazole **(C)**, and quinazoline fused 1,2,4-triazole **(D)** based medicinal active molecules

1,2,4-Triazole is also an imperative nitrogen heterocyclic pharmacophore[18, 19]that can effectively form H-bonding with biological targets, which would be advantageous to enhance its biological efficacy. The 1,2,4-triazole containing molecules recently reported with anti-fungal[20], antibacterial[21], anticancer (PARP-1 inhibitor)[22-24] and anti-inflammatory[25]. These structural features and biomedicinal potential in numerous biological activities have made this scaffold very imperative in drug discovery.

Currently, molecular hybridization is being utilized as a trending approach for the development of hybrid heterocycles with boosted (i) potency (ii) pharmacokinetic profile, (iii) selectivity (iv) multiple modes of action, and (v) manifold activities. In this scenario, molecular hybridization of quinazoline scaffold with different bioactive pharmacophores resulted in lead compounds with multi-faceted biological activity, wherein specific as well as multiple targets were involved[16]. Moreover, would

offer a better pharmacological effect compared to quinazoline and triazoles alone. Also, fused 1,2,4-triazoloquinazoline pharmacophore is well-recognized for numerous fascinating bioactivities[26]for examples antibacterial[27], antihypertensive[28,29], anticonvulsant[30,31], antimalarial[32], antioxidant[33],EGFR inhibitor[17],α-glucosidase inhibitor[34], antiproliferative[35], antiviral[36], antimicrobial[37,38], and anti-inflammatory[39, 40]. Recently, Abulkhair and other researchers disclosed the synthesis and anticancer potential of 1,2,4-triazoloquinazolines[41-46].Therefore, inspired by molecular-hybridization results[47],and the excellent antiproliferative and antioxidant profile of this hybrid molecule, reported by our group[48],the present work continues to explore the mild synthesis of some quinazoline-triazole hybrids molecules.

Experimental Section

Materials and Methods

Melting points were taken in open capillaries on an electrical apparatus and which may be uncorrected. ^{1}H NMR (400 and 500 MHz) and ^{13}C NMR (100 and 125 MHz) were recorded on Advance III, 400 MHz Bruker and JNM ECX (Jeol India) 500 MHz spectrophotometer using $CDCl_3$ or DMSO-d_6 as solvent according to solubility of compound. IR spectra (KBr) were recorded on Perkin-Elmer IR spectrophotometer in the range of 400-4000 cm^{-1}. The standard compound, being a purified compound and highly active substance, was assessed using a lower concentration range (0 to 50 µg/mL). In contrast, the sample's potency remains unbound; therefore, a broader concentration range (0 to 1000 µg/mL) was employed for the sample analysis.

Procedure for synthesis of 3-aryl-5-phenyl-[1,2,4]triazolo[4,3-c]quinazolines, 5a-n

To a well-stirred solution of (*E*)-4-(2-(4-nitrobenzylidene)hydrazinyl)-2-phenylquinazoline **(4n)** (1.0 mmol, 369.38 mg, 1.0 equiv.) in dichloromethane (25-30 mL) at RT, iodobenzenediacetate (1.1 mmol, 354.31 mg, 1.1 equiv.) was added slowly in four to five portions during 5 min. The resulting reaction mixture was then allowed to stir continuously for 2 h at RT. The reaction was monitored periodically by TLC and after completion of reaction, the dichloromethane was evaporated on a steam bath. The brown coloured residual mass containing desired products and iodobenzene was then triturated two or three times with petroleum-ether to remove iodobenzene as by-product. Resulting yellow coloured solid residue was then recrystallized by ethanol and identified as 3-(4-nitrophenyl)-5-phenyl-[1,2,4]triazolo [4,3-c]quinazoline **(5n)** in isolated yield of 80% (0.80 mmol, 283 mg,). There was no requirement of column chromatography.

Antiproliferative Activity

The cytotoxic potential of compounds **5a-5n** were determined by means of MTT (3-(4,5-dimethylthiazol-2-yl)-2,5-diphenyltetrazolium bromide) assay with slight modifications[67].In this experiment, cells were seeded in 96 well microplates at the concentration of 8×103 cells/0.1 mL of media and incubated to allow cell attachment. After 24 h, cells were treated with different concentrations (31.25-500 µM) of the compound using serial dilutions method. On the completion of total 48 h, 20 µL of MTT was added to each well. Thereafter, the ability of viable cells to reduce it into insoluble purple coloured formazan was measured and the cells were further incubated for 3 h. After this, removed the supernatant containing MTT solution from each well and the intracellular MTT formazan was dissolved in 100 µL of DMSO. Finally, the decrease in absorbance was measured at 570 nm using a multiwell plate reader (BioTek Synergy HT). The percentage growth inhibition was calculated using the formula:% Growth inhibition = A0-A1/A0×100, where, A0 is the absorbance of control, A1 is the absorbance of test sample.

Molecular Docking

Molecular docking studies were carried out to better understand the specific binding site of the different synthesized compounds in the protein environment and investigate the binding behaviour of the ligands. The compounds' three-dimensional (3D) structures were drawn using molecular operating environment (MOE) and energy-optimized using the AM1 semi-empirical approach with an RMS gradient of 0.001 $kcalmol^{-1}$. Protein Data Bank was used to download the crystal structure of 3u6j. Before docking, the suitable binding sites for inserting the ligands in the active sites of 3u6j were determined by the site finder, and a total of 16 binding sites in 3u6j were discovered in the process. Finally, the compounds were docked to the favourable site of 3u6j determined by MOE's using the Alfa PMI placement approach, and the best fitting domain was chosen for the docking research.

Antioxidant Activity

ABTS (SRL-Chem-Cat no.-28042) radicals were prepared by mixing APS (2.45 mM) and ABTS (7mM) solution, which was diluted 100X to prepare ABTS free radical reagent[68-70]. 10µl of different stock of the standard (Ascorbic Acid -SD Fine-F13A/0413/1106/62, Concentration as per mentioned in excel sheet) and samples (as per mentioned in excel sheet) were added to 200µl of ABTS free radical reagent in 96 well plate and incubated at RT for 10 min in dark. The wells without treatment were considered as control. After incubation, the absorbance of the de-colorization at 750nm is measured using a microplate reader (iMark, BioRad). Results were presented with respect to negative control. IC50 was calculated using Software Graph Pad Prism 9.5.1. Graph was prepared between X axis (Sample Concentration) *vs*. Y axis (% inhibition w.r.t. control).

Characterization data for 4-Hydrazinyl-2-phenylquinazoline, 2

Yellow solid. Yield 85%. m.p. 188-190°C. R_f = 0.5 (ethyl acetate/pet-ether, 6:4); ^{1}H NMR (400 MHz, DMSO-d_6, 25°C, TMS): δ_H = 9.703 (bs, 1H, N-H), 8.612-8.601 (d, ^3J = 4.4 Hz, 2H, CH_{Ar}), 8.240-8.220 (d, ^3J = 8.0 Hz, 1H, CH_{Ar}), 7.801-7.739 (m, 2H, CH_{Ar}), 7.532-7.460 (m, 5H, CH_{Ar}), 4.959 (bs, 2H, NH_2); ^{13}C NMR (100 MHz, DMSO-d_6, 25°C, TMS): δc = 160.42, 159.74, 150.01, 139.08, 133.11, 130.60, 128.66, 128.62, 128.23, 125.78, 122.80, 113.38.

Characterization data for (E)-4-(2-benzylidenehydrazinyl)-2-phenylquinazoline derivatives, 4a-n

(E)-4-(2-(3-Methylbenzylidene)hydrazinyl)-2-phenylquinazoline, 4b: Greenish solid. Yield 74%. R_f = 0.47 (ethyl acetate/*n*-hexane, 2:8); ^{1}H NMR (400 MHz, DMSO-d_6, 25°C, TMS): δ_H = 11.803 (s, 1H, N=C-H), 8.767 (bs, 1H, N-H), 8.584-8.493 (m, 3H, CH_{Ar}), 7.903-7.854 (m, 2H, CH_{Ar}), 7.684-7.665 (d, ^3J = 7.6 Hz, 1H, CH_{Ar}), 7.639-7.528 (m, 5H, CH_{Ar}), 7.436-7.398 (m,1H, CH_{Ar}), 7.294-7.276 (d, ^3J = 8.0 Hz, 1H, CH_{Ar}) 2.412 (s, 3H, CH_3); ^{13}C NMR (100 MHz, DMSO-d_6, 25°C, TMS): δc = 159.74, 146.48, 138.72, 138.69, 135.04, 133.78, 132.03, 131.09, 130.84, 129.45, 129.43, 128.90, 128.55, 128.52, 128.22, 126.39, 126.35, 124.44, 113.28, 21.53; HRMS: *m/z* $[M+H]^+$ Calcd for $C_{22}H_{18}N_4$: 339.1559. Found: 339.1800.

(E)-2-Phenyl-4-(2-(2,3,4-trimethoxybenzylidene)hydrazinyl)quinazoline, 4g: Pale solid. Yield 92%. m.p. 124-130°C. R_f = 0.62 (ethyl acetate/*n*-hexane, 2:8);^{1}H NMR (400 MHz, DMSO-d_6, 25°C, TMS): δ_H = 11.748 (s, 1H, N=C-H), 8.738 (bs, 1H, N-H), 8.775-8.563 (m, 3H, CH_{Ar}), 7.887-7.837 (m, 2H, CH_{Ar}), 7.801-7.779 (d, ^3J = 8.8 Hz, 1H, CH_{Ar}), 7.614-7.522 (m, 4H, CH_{Ar}), 7.044-7.022 (d, ^3J = 8.8 Hz, 1H, CH_{Ar}), 3.920 (s, 3H, OCH_3), 3.887 (s, 3H, OCH_3), 3.819 (s, 3H, OCH_3); ^{13}C NMR (100 MHz, DMSO-d_6, 25°C, TMS): δc = 159.78, 159.74, 155.48, 152.99, 151.72, 142.21, 142.15, 138.77, 133.66, 130.79, 130.70, 128.85, 128.48, 128.38, 128.32, 126.18, 121.30, 121.05, 109.46, 62.39, 61.06, 56.56; HRMS: *m/z* $[M+H]^+$ Calcd for $C_{24}H_{22}N_4O_3$: 415.1759. Found: 415.2012.

(E)-2-Phenyl-4-(2-(4-(trifluoromethyl)benzylidene)hydrazinyl) quinazoline, 4l: Pale yellow solid. Yield 90%. m.p. 190-196°C. R_f = 0.41 (ethyl acetate/*n*-hexane, 2:8); IR ($\bar{\upsilon}_{max}$, KBr, cm^{-1}): No peak in N-H region, 3247 (N-H stretching), 1549 (C=N)arom.; ^{1}H NMR (400 MHz, DMSO-d_6, 25°C, TMS): δ_H = 12.021 (s, 1H, N=C-H), 8.737 (bs, 1H, N-H), 8.596-8.577 (d, ^3J = 7.6 Hz, 3H, CH_{Ar}), 8.073-8.053 (d, ^3J = 8.0 Hz, 2H, CH_{Ar}), 7.909-7.869 (m, 4H, CH_{Ar}), 7.656-7.621 (m, 1H, CH_{Ar}), 7.566-7.550 (m, 3H, CH_{Ar}); ^{13}C NMR (100 MHz, DMSO-d_6, 25°C, TMS): δc = 159.67, 144.52, 139.11, 134.02, 133.94, 130.94, 128.92, 128.59, 128.54, 127.97, 126.58, 126.56, 126.41, 126.36, 126.06, 123.36, 113.26, 95.99; HRMS: *m/z* $[M+H]^+$ Calcd for $C_{22}H_{15}F_3N_4$: 393.1259. Found: 393.1322.

Characterization data for 3-aryl-5-phenyl-[1,2,4]triazolo[4,3-c]quinazolines, 5a-n

3-(2-Methylphenyl)-5-phenyl-[1,2,4]triazolo[4,3-c]quinazoline, 5a: Mustered solid. Yield 55% (0.55 mmol, 185 mg). m.p. 162-164°C. R_f = 0.23 (ethyl acetate/pet-ether, 3:7); IR ($\bar{\upsilon}_{max}$, KBr, cm^{-1}): No peak in N-H region, 3247 (N-H stretching), 1549 (C=N)arom.; ^{1}H NMR (400 MHz, DMSO-d_6, 25°C, TMS): δ_H = 8.632-8.614 (dd, ^3J = 6.4 Hz, ^5J = 0.8 Hz, 1H, CH_{Ar}), 8.024-8.009 (d, ^3J = 6.0 Hz, 1H, CH_{Ar}), 7.925-7.891 (dt, ^3J = 6.4 Hz, ^5J = 1.2 Hz, 1H, CH_{Ar}), 7.857-7.824 (dt, ^3J = 6.4 Hz, ^5J = 1.2 Hz, 1H, CH_{Ar}), 7.392-7.375 (m, 2H, CH_{Ar}), 7.224-7.190 (m, 1H, CH_{Ar}), 7.147-7.115 (m, 1H, CH_{Ar}), 7.072-7.007 (m, 4H, CH_{Ar}), 6.907-6.878 (t, ^3J = 6.0 Hz, 1H, CH_{Ar}), 2.060 (s, 3H, CH_3);^{13}C NMR (100 MHz, DMSO-d_6, 25°C, TMS): δc = 148.62, 147.12, 146.02, 144.93,

140.63, 136.92, 131.84, 131.71, 130.94, 129.68, 129.30, 129.09, 128.63, 127.93, 127.58, 126.87, 124.78, 122.48, 116.09, 19.51; HRMS: *m/z* $[M+H]^+$ Calcd for $C_{22}H_{16}N_4$: 337.1459. Found: 337.1426.

3-(3-Methylphenyl)-5-phenyl-[1,2,4]triazolo[4,3-c]quinazoline, 5b: Brown solid. Yield 54% (0.54 mmol, 182 mg). m.p. 189-191°C. R_f = 0.23 (ethyl acetate/pet-ether, 3:7); IR ($\bar{\upsilon}_{max}$, KBr, cm^{-1}): No peak in N-H region, 3247 (N-H stretching), 1549 (C=N)arom.; ^{1}H NMR (500 MHz, DMSO-d_6, 25°C, TMS): δ_H =8.777-8.754 (m, 1H, CH_{Ar}),8.050-8.026 (m, 1H, CH_{Ar}), 7.837-7.797 (m, 1H, CH_{Ar}), 7.767-7.728 (m, 1H, CH_{Ar}), 7.339-7.299 (m, 2H, CH_{Ar}), 7.279-7.255 (m, 2H, CH_{Ar}), 7.141-7.094 (m, 2H, CH_{Ar}), 7.052-7.022 (m, 2H, CH_{Ar}), 6.901-6.879 (m, 1H, CH_{Ar}); ^{13}C NMR (125 MHz, $CDCl_3$, 25°C, TMS): δc =149.05, 145.71, 141.12, 139.53, 137.52, 131.98, 130.46, 130.40, 130.27, 130.18, 129.39, 128.87, 128.65, 128.47, 127.86, 127.84, 127.80, 126.70, 123.64, 20.96; HRMS: *m/z* $[M+H]^+$ Calcd for $C_{22}H_{16}N_4$: 337.1459. Found: 337.1426.

3-(4-Methylphenyl)-5-phenyl-[1,2,4]triazolo[4,3-c]quinazoline, 5c: Off white solid. Yield 58% (0.58 mmol, 195 mg). m.p. 140-142°C. R_f = 0.28 (ethyl acetate/pet-ether, 3:7); IR ($\bar{\upsilon}_{max}$, KBr, cm^{-1}): No peak in N-H region, 3247 (N-H stretching), 1549 (C=N)arom.; ^{1}H NMR (400 MHz, DMSO-d_6, 25°C, TMS): δ_H = 8.612-8.589 (dd, ^3J = 8.0 Hz, ^5J = 1.2 Hz, 1H, CH_{Ar}), 8.025-8.003 (dd, ^3J = 8.0 Hz, ^5J = 0.8 Hz, 1H, CH_{Ar}), 7.914-7.872 (m, 1H, CH_{Ar}), 7.838-7.797 (m, 1H, CH_{Ar}), 7.754-7.730 (m, 1H, CH_{Ar}), 7.405-7.373 (m, 2H, CH_{Ar}), 7.296-7.253 (m, 1H, CH_{Ar}), 7.209-7.170 (m, 1H, CH_{Ar}), 7.116-7.077 (m, 2H, CH_{Ar}), 6.910-6.891 (d, ^3J = 7.6 Hz, 2H, CH_{Ar}), 2.228 (s, 3H, CH_3); ^{13}C NMR (100 MHz, DMSO-d_6, 25°C, TMS): δc = 149.53, 149.13, 146.72, 141.23, 138.97, 137.64, 132.27, 131.20, 130.25, 129.93, 129.61, 128.42, 128.23, 127.72, 125.50, 123.09, 116.64, 21.58; HRMS: *m/z* $[M+H]^+$ Calcd for $C_{22}H_{16}N_4$: 337.1459. Found: 337.1426.

3-(4-Isopropylphenyl)-5-phenyl-[1,2,4]triazolo[4,3-c]quinazoline, 5d: Light orange solid. Yield 77% (0.77 mmol, 281 mg). m.p. 164-166°C. R_f = 0.16 (ethyl acetate/pet-ether, 3:7); IR ($\bar{\upsilon}_{max}$, KBr, cm^{-1}): No peak in N-H region, 3247 (N-H stretching), 1549 (C=N)arom.; ^{1}H NMR (500 MHz, DMSO-d_6, 25°C, TMS): δ_H = 8.611-8.593 (dd, ^3J = 8.0 Hz, ^5J = 1.0 Hz,1H, CH_{Ar}), 8.020-8.005 (d, ^3J = 7.5 Hz,1H, CH_{Ar}), 7.910-7.876 (dt, ^3J = 7.0 Hz, ^5J = 1.5 Hz,1H, CH_{Ar}), 7.836-7.803 (m,1H, CH_{Ar}), 7.347-7.329 (m, 2H, CH_{Ar}), 7.241-7.207 (m,1H, CH_{Ar}), 7.107-7.091 (d, ^3J = 8.0 Hz, 2H, CH_{Ar}), 7.071-7.040 (m, 2H, CH_{Ar}), 6.941-6.925 (d, ^3J = 8.0 Hz, 2H, CH_{Ar}), 2.838-2.755 (s, ^3J = 7.0 Hz, 1H, CH), 1.158-1.145 (d, ^3J = 6.5 Hz, 6H, $(CH_3)_2$); ^{13}C NMR (125 MHz, DMSO-d_6, 25°C, TMS): δc = 149.28, 148.84, 148.48, 146.13, 140.61, 132.32, 131.64, 129.58, 129.45, 129.00, 128.94, 127.87, 127.00, 125.16, 122.46, 116.05, 33.19, 23.57; HRMS: *m/z* $[M+H]^+$Calcd for $C_{24}H_{20}N_4$: 365.1759; found: 365.1784.

4-(5-Phenyl-[1,2,4]triazolo[4,3-c]quinazolin-3-yl)phenol, 5e: Brown solid. Yield 56% (0.56 mmol, 181 mg). m.p. 220-222°C. R_f = 0.38 (ethyl acetate/pet-ether, 3:7); IR ($\bar{\upsilon}_{max}$, KBr, cm^{-1}): No peak in N-H region, 3247 (N-H stretching), 1549 (C=N)arom.; ^{1}H NMR (500 MHz, DMSO-d_6, 25°C, TMS): δ_H =9.645 (s, 1H, OH),8.594-8.575 (dd, ^3J = 8.0 Hz, ^5J = 1.5 Hz, 1H, CH_{Ar}), 8.010-7.995 (d, ^3J = 7.5 Hz, 1H, CH_{Ar}), 7.898-7.865 (dt, ^3J = 7.0 Hz, ^5J = 1.5 Hz, 1H, CH_{Ar}), 7.823-7.790 (m, 1H, CH_{Ar}), 7.399-7.380 (d, ^3J = 8.5 Hz, 2H, CH_{Ar}),7.321-7.286 (m, 1H, CH_{Ar}), 7.155-7.124 (m,2H, CH_{Ar}), 7.030-7.002 (d, ^3J = 8.5 Hz, 2H, CH_{Ar}), 6.475-6.447 (d, ^3J = 8.5 Hz, 2H, CH_{Ar}); ^{13}C NMR (125 MHz, DMSO-d_6, 25°C, TMS): δc = 157.92, 148.68, 146.22, 140.55, 132.51, 131.54, 130.84, 129.69, 129.05, 128.93, 127.82, 127.06, 122.40, 118.20, 116.08, 114.15, 111.72; HRMS: *m/z* $[M+H]^+$ Calcd for $C_{21}H_{14}N_4O$; 339.1259. Found: 339.1201.

3-(4-Methoxyphenyl)-5-phenyl-[1,2,4]triazolo[4,3-c]quinazoline, 5f: White solid. Yield 60% (0.60 mmol, 211 mg). m.p. 228-230°C. R_f = 0.34 (ethyl acetate/pet-ether, 3:7); IR ($\bar{\upsilon}_{max}$, KBr, cm^{-1}): No peak in N-H region, 3247 (N-H stretching), 1549 (C=N)arom.; ^{1}H NMR (500 MHz, $CDCl_3$, 25°C, TMS): δ_H = 8.774-8.759 (dd, ^3J = 5.2 Hz, ^5J = 0.8 Hz, 1H, CH_{Ar}), 8.043-8.026 (dd, ^3J = 6.4 Hz, ^5J = 0.4 Hz, 1H, CH_{Ar}), 7.831-7.797 (m, 1H, CH_{Ar}), 7.761-7.729 (m, 1H, CH_{Ar}), 7.328-7.296 (m, 2H, CH_{Ar}), 7.283-7.278 (m, 1H, CH_{Ar}), 7.161-7.130 (m, 2H, CH_{Ar}), 7.098-7.080 (dd, ^3J = 5.2 Hz, ^5J = 1.6 Hz, 2H, CH_{Ar}), 6.625-6.607 (dd, ^3J = 5.6 Hz, ^5J = 1.6 Hz, 2H, CH_{Ar}), 3.765 (s, 3H, OCH3);^{13}C NMR (100 MHz, $CDCl_3$, 25°C, TMS): δc = 160.48, 149.64, 148.78, 145.70, 141.10, 132.29, 132.02, 130.93, 130.43, 129.35, 128.94, 128.33, 127.89, 123.68, 119.68, 116.12, 113.40, 55.39; HRMS: *m/z* $[M+H]^+$ Calcd for $C_{22}H_{16}N_4O$: 353.1359. Found: 353.1373.

5-Phenyl-3-(2,3,4-trimethoxyphenyl)-[1,2,4]triazolo[4,3-c]quinazoline, 5g: White solid. Yield 82% (0.82 mmol, 338 mg). m.p. 178-180°C. R_f = 0.33 (ethyl acetate/pet-ether, 3:7); IR ($\bar{\upsilon}_{max}$, KBr, cm^{-1}): No peak in N-H region, 3247 (N-H stretching), 1549 (C=N)arom.; ^{1}H NMR (500 MHz, DMSO-d_6, 25°C, TMS): δ_H = 8.765-8.747 (dd, ^3J = 8.0 Hz, ^5J = 1.0 Hz, 1H, CH_{Ar}), 8.045-8.027 (dd, ^3J = 8.0 Hz, ^5J = 1.0 Hz, 1H, CH_{Ar}), 7.829-7.795 (dt, ^3J = 7.5 Hz, ^5J = 1.5 Hz, 1H, CH_{Ar}), 7.757-7.724 (dt, ^3J = 8.0 Hz, ^5J = 1.0 Hz, 1H, CH_{Ar}),7.278-7.243 (m, 3H, CH_{Ar}), 7.202-7.185 (d, ^3J = 8.5 Hz, 1H, CH_{Ar}), 7.142-7.112 (m, 2H, CH_{Ar}), 6.650-6.633 (d, ^3J = 8.5 Hz, 1H, CH_{Ar}), 3.851 (s, 3H, OCH_3), 3.510 (s, 3H, OCH_3), 3.443 (s, 3H, OCH_3); ^{13}C NMR (125 MHz, DMSO-d_6, 25°C, TMS): δc = 155.20, 150.52, 148.67, 146.34, 145.36, 140.48, 140.23, 131.75, 131.64, 129.70, 129.08, 128.90, 127.94, 126.59, 125.62, 122.46, 115.79, 115.00, 107.43, 60.47, 60.23, 56.00; HRMS: *m/z* $[M+H]^+$ Calcd for $C_{24}H_{20}N_4O_3$ 413.1559. Found: 413.1584.

3-(4-Fluorophenyl)-5-phenyl-[1,2,4]triazolo[4,3-c]quinazoline, 5h: White solid. Yield 68% (0.68 mmol, 231 mg). m.p. 208-210°C. R_f = 0.41 (ethyl acetate/pet-ether, 3:7); IR ($\bar{\upsilon}_{max}$, KBr, cm^{-1}): No peak in N-H region, 3247 (N-H stretching), 1549 (C=N)arom.; ^{1}H NMR (500 MHz, $CDCl_3$, 25°C, TMS): δ_H = 8.783-8.765 (dd, ^3J = 6.0 Hz, ^5J = 0.8 Hz, 1H, CH_{Ar}), 8.056-8.039 (dd, ^3J = 6.4 Hz, ^5J = 0.8 Hz, 1H, CH_{Ar}), 7.852-7.818 (m, 1H, CH_{Ar}), 7.781-7.749 (m, 1H, CH_{Ar}), 7.349-7.304 (m, 3H, CH_{Ar}), 7.183-7.138 (m, 4H, CH_{Ar}), 6.829-6.782 (m, 2H, CH_{Ar}); ^{13}C NMR (100 MHz, DMSO-d_6, 25°C, TMS): δc = 162.96, 160.93, 148.97, 148.92, 145.98, 140.63, 132.36, 131.88, 131.79, 131.75, 129.79, 129.11, 129.06, 127.89, 127.19, 124.38, 124.34, 122.48, 115.98, 114.43, 114.22; HRMS: *m/z* $[M+H]^+$ Calcd for $C_{21}H_{13}FN_4$: 341.1159. Found: 341.1196.

3-(4-Chlorophenyl)-5-phenyl-[1,2,4]triazolo[4,3-c]quinazoline, 5i: Off white solid. Yield 75% (0.75 mmol, 268 mg). m.p. 216-218°C. R_f = 0.22 (ethyl acetate/pet-ether, 3:7); IR ($\bar{\upsilon}_{max}$, KBr, cm^{-1}): No peak in N-H region, 3247 (N-H stretching), 1549 (C=N)arom.; ^{1}H NMR (500 MHz, $CDCl_3$, 25°C, TMS): δ_H = 8.768-8.750 (dd, ^3J = 6.4 Hz, ^5J = 0.8 Hz, 1H, CH_{Ar}), 8.112-8.070 (m, 2H, CH_{Ar}), 7.889-7.855 (m, 1H, CH_{Ar}), 7.830-7.747 (m, 3H, CH_{Ar}), 7.435-7.403 (t, ^3J = 6.4 Hz, 1H, CH_{Ar}), 7.357-7.338 (dd, ^3J = 6.4 Hz, ^5J = 0.8 Hz, 2H, CH_{Ar}), 7.275-7.240 (m, 1H, CH_{Ar}), 7.157-7.126 (m, 2H, CH_{Ar});^{13}C NMR (125 MHz, $CDCl_3$, 25°C, TMS): δc =140.42, 137.04, 135.27, 133.12, 132.47, 132.04, 131.39, 130.69, 130.35, 129.95, 129.62, 128.98, 128.10, 128.05, 128.01, 126.90, 122.15; HRMS: *m/z* $[M+H]^+/[M+H+2]^+$ Calcd for $C_{21}H_{13}ClN_4$: 357.0859/359.0859. Found: 357.0903/359.0885.

3-(2,3-Dichlorophenyl)-5-phenyl-[1,2,4]triazolo[4,3-c]quinazoline, 5j: Off white solid. Yield 76% (0.76 mmol, 297 mg). m.p. 188-190°C. R_f = 0.23 (ethyl acetate/pet-ether, 3:7); IR ($\bar{\upsilon}_{max}$, KBr, cm^{-1}): No peak in N-H region, 3247 (N-H stretching), 1549 (C=N)arom.; ^{1}H NMR (400 MHz, DMSO-d_6, 25°C, TMS): δ_H = 8.659-8.640 (d, ^3J = 7.6 Hz, 1H, CH_{Ar}), 8.065-8.045 (d, ^3J = 8.0 Hz, 1H, CH_{Ar}), 7.966-7.926 (m, 1H, CH_{Ar}), 7.895-7.857 (m, 1H, CH_{Ar}), 7.584-7.564 (d, ^3J = 8.0 Hz, 2H, CH_{Ar}), 7.494-7.481 (m, 2H, CH_{Ar}), 7.372-7.333 (d, ^3J = 7.6 Hz, 1H, CH_{Ar}), 7.308-7.270 (t, ^3J = 7.6 Hz, 1H, CH_{Ar}), 7.212-7.136 (m, 2H, CH_{Ar}); ^{13}C NMR (100 MHz, DMSO-d_6, 25°C, TMS): δc = 149.58, 146.14, 145.51, 141.25, 132.78, 132.51, 132.12, 132.00, 131.92, 131.66, 130.76, 130.41, 130.09, 129.45, 128.74, 128.62, 127.33, 123.27, 116.33; HRMS: *m/z* $[M+H]^+/[M+H+2]^+/[M+H+4]^+$ Calcd for $C_{21}H_{12}Cl_2N_4$: 391.0459/393.0459/395.0459. Found: 391.0515/393.0489/394.0493.

3-(Naphthalen-1-yl)-5-phenyl-[1,2,4]triazolo[4,3-c]quinazoline, 5k: Off white solid. Yield 80% (0.80 mmol, 298 mg). m.p. 124-126°C. R_f = 0.28 (ethyl acetate/pet-ether, 3:7); IR ($\bar{\upsilon}_{max}$, KBr, cm^{-1}): No peak in N-H region, 3247 (N-H stretching), 1549 (C=N)arom.; ^{1}H NMR (500 MHz, DMSO-d_6, 25°C, TMS): δ_H = 8.846-8.828 (dd, ^3J = 8.0 Hz, ^5J = 1.5 Hz, 1H, CH_{Ar}), 8.055-8.038 (dd, ^3J = 8.0 Hz, ^5J = 1.0 Hz, 1H, CH_{Ar}), 7.865-7.831 (m, 1H, CH_{Ar}), 7.811-7.778 (m, 1H, CH_{Ar}), 7.728-7.694 (m, 2H, CH_{Ar}), 7.440-7.407 (m, 1H, CH_{Ar}), 7.395-7.347 (m, 3H, CH_{Ar}), 7.269-7.239 (m, 1H, CH_{Ar}), 7.010-6.995 (d, ^3J = 7.5 Hz, 2H, CH_{Ar}), 6.929-6.894 (m, 1H, CH_{Ar}), 6.691-6.663 (m, 2H, CH_{Ar});^{13}C NMR (100 MHz, DMSO-d_6, 25°C, TMS): δc = 149.02, 146.52, 146.01, 140.73, 132.28, 131.76, 131.71, 131.33, 129.73, 129.65, 129.25, 129.08, 127.99, 127.93, 127.72, 126.58, 126.04, 125.92, 125.20, 125.18, 124.38, 122.55, 116.22; HRMS: *m/z* $[M+H]^+$ Calcd for $C_{25}H_{16}N_4$: 373.1459. Found: 373.1460.

5-Phenyl-3-(4-(trifluoromethyl)phenyl)-[1,2,4]triazolo[4,3-c]quinazoline: **5l**: White solid. Yield 81% (0.81 mmol, 316 mg). m.p. 238-240°C. R_f = 0.62 (ethyl acetate/pet-ether, 3:7); IR ($\bar{\upsilon}_{max}$, KBr,

cm^{-1}): No peak in N-H region, 3247 (N-H stretching), 1549 (C=N)arom.; ^{1}H NMR (400 MHz, DMSO-d_6, 25°C, TMS): δ_H = 8.633-8.611 (dd, ^3J = 8.0 Hz, ^5J = 0.8 Hz, 1H, CH_{Ar}), 8.044-8.024 (m, 1H, CH_{Ar}), 7.939-7.897 (d, ^3J = 8.5 Hz, 2H, CH_{Ar}), 7.862-7.821 (d, 3J = 8.0 Hz, 1H, CH_{Ar}), 7.480-7.398 (m, 6H, CH_{Ar}), 7.272-7.234 (t, ^3J = 7.6 Hz, 1H, CH_{Ar}), 7.113-7.075 (m, 2H, CH_{Ar}); ^{13}C NMR (100 MHz, DMSO-d_6, 25°C, TMS): δc = 149.89, 147.85, 146.40, 141.34, 132.92, 132.53, 130.90, 130.43, 129.79, 129.71, 128.56, 127.88, 125.76, 124.69, 124.65, 123.19, 116.51; HRMS: *m/z* $[M+H]^+$ Calcd for $C_{22}H_{13}F_3N_4$: 391.1159. Found: 391.1163.

3-(3-Nitrophenyl)-5-phenyl-[1,2,4]triazolo[4,3-c]quinazoline, 5m: White solid. Yield 86% (0.86 mmol, 320 mg). m.p. 250-252°C. R_f = 0.81 (ethyl acetate/pet-ether, 3:7); IR ($\bar{\upsilon}_{max}$, KBr, cm^{-1}): No peak in N-H region, 3247 (N-H stretching), 1549 (C=N)arom.; ^{1}H NMR (500 MHz, $CDCl_3$, 25°C, TMS): δ_H = 8.799-8.781 (dd, ^3J = 6.4 Hz, ^5J = 0.8 Hz, 1H, CH_{Ar}), 8.112-8.070 (m, 2H, CH_{Ar}), 7.889-7.855 (m, 1H, CH_{Ar}), 7.830-7.747 (m, 3H, CH_{Ar}), 7.435-7.403 (t, ^3J = 6.4 Hz, 1H, CH_{Ar}), 7.357-7.338 (dd, ^3J = 6.4 Hz, ^5J = 0.8 Hz, 2H, CH_{Ar}), 7.275-7.240 (m, 1H, CH_{Ar}), 7.157-7.126 (m, 2H, CH_{Ar});^{13}C NMR (100 MHz, $CDCl_3$, 25°C, TMS): δc = 148.87, 143.86, 143.68, 143.64, 143.62, 138.58, 137.12, 133.91, 133.28, 131.06, 131.04, 129.08, 128.98, 128.92, 128.52, 128.01, 126.51, 124.42, 121.61; HRMS: *m/z* $[M+H]^+$ Calcd for $C_{21}H_{13}N_5O_2$: 368.1159. Found: 368.1142.

3-(4-Nitrophenyl)-5-phenyl-[1,2,4]triazolo[4,3-c]quinazoline, 5n: Off white solid. Yield 88% (0.88 mmol, 323 mg). m.p. 260-262°C. R_f = 0.63 (ethyl acetate/pet-ether, 3:7); IR ($\bar{\upsilon}_{max}$, KBr, cm^{-1}): No peak in N-H region, 3247 (N-H stretching), 1549 (C=N)arom.; ^{1}H NMR (500 MHz, $CDCl_3$, 25°C, TMS): δ_H = 8.607-8.583 (dd, ^3J = 8.0 Hz, ^5J = 1.2 Hz, 1H, CH_{Ar}), 8.018-7.997 (m, 1H, CH_{Ar}), 7.922-7.869 (m, 3H, CH_{Ar}), 7.832-7.791 (m, 1H, CH_{Ar}), 7.509-7.475 (m, 2H, CH_{Ar}), 7.416-7.393 (m, 2H, CH_{Ar}), 7.256-7.213 (m, 1H, CH_{Ar}), 7.107-7.069 (m, 2H, CH_{Ar});^{13}C NMR (100 MHz, DMSO-d_6, 25°C, TMS): δc = 150.10, 147.68, 147.40, 146.30, 141.40, 134.98, 133.00, 132.63, 131.43, 130.72, 129.85, 129.76, 128.59, 128.05, 123.23, 122.80, 116.46; HRMS: *m/z* $[M+H]^+$ Calcd for $C_{21}H_{13}N_5O_2$: 368.1159. Found: 368.1142.

Results and Discussion

Synthetic Chemistry

We commenced our work with preparation of 4-hydrazineyl-2-phenylquinazoline **2** from 2-3 h refluxing of commercially available 4-chloro-2-phenylquinazoline **1** with excess of hydrazine hydrate in C_2H_5OH (20-25 mL) as solvent (Scheme 1). Thereafter, key quinazoline hydrazine (1.0 equiv.) has been condensed with various aryl aldehydes (1.0 equiv.) in C_2H_5OH-CH_3COOH (cat.) solvent system according to our recently published report[49,50].The reaction undergoes smoothly, both in case of electron-donating (–CH_3, –OCH_3, 3,4-OCH_3, –$CH(CH_3)_2$) as well as electron-withdrawing (–F, –Cl, –Br, –NO_2, –CF_3) substituted benzaldehydes (yield = 50-85%). Finally. Fourteen quinazoline-hydrazone derivatives **4a-n** were successfully synthesized, and subsequently then subjected to oxidative-cyclization with iodobenzene diacetate (1.1 equiv.) to explore the reaction scope for quinazoline-triazole[41].The reaction was carried out under stirring for 2-3 hours at RT in

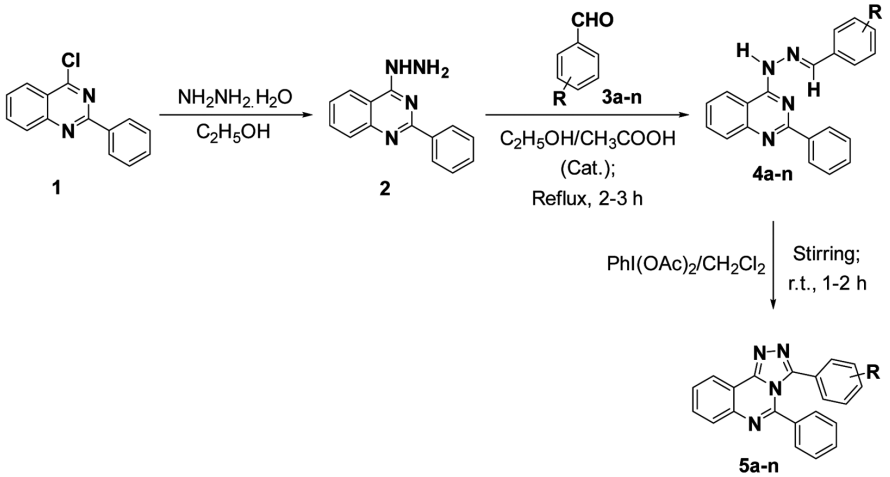

Scheme 1 — Synthesis of 3-aryl-5-phenyl-[1,2,4]triazolo[4,3-c]quinazolines

dichloromethane (20 mL) as solvent[51].After 2-3 hours continuous stirring, it has been observed from TLC that quinazoline-hydrazones were consumed completely. Then after the solvent evaporation, crude product was triturated two-three with petroleum-ether to remove iodobenzene (by product). The obtained solid residue was then recrystallised with ethanol. Finally, the target quinazoline-triazoles were isolated as pure compounds in 54-88% yield range.

The expected structure of obtained solid yellow coloured product *i.e.*, 5-phenyl-3-(4-(trifluoro-methyl)phenyl)-[1,2,4]triazolo[4,3-c]quinazoline **(5l)** has been proposed by careful analysis of spectroscopic characterization data (IR, ^{1}H & ^{13}C NMR) and satisfactory HRMS data (Fig. 2).Initially, loss of N-H stretching frequency nearly at 3227 cm^{-1} in IR spectra, exposes the oxidative cyclization of **4l** into corresponding triazole **5l**. In addition, loss of one broad singlet at 8.737 ppm and one simple singlet at 12.021 ppm due to the presence of H-N-N=and -N=C-H fragments, respectively of hydrazone in ^{1}H NMR spectrum of **5l**, strongly indicates the oxidative-cyclization of quinazoline-hydrazone **4l** to quinazoline-triazole **5l**. Likewise, ^{13}C NMR spectrum of both **4l** and **5l** exhibits seventeen different resonating signals in their expected aromatic region. Notably, the ^{13}C signal of alkene (-N-N=C-H) at 113.26 ppm shifted to the aromatic region after cyclization. The *m/z* $[M+H]^+$ value for triazole **5l** was greatly coincided (found. 391.1163) with the expected value (Calcd. 391.1159) which was expectedly lesser by 2 unit from corresponding hydrazone (Calcd. 393.1259; found 393.1322).

Antiproliferative Activities

Newly synthesized compounds 3-aryl-5-phenyl-[1,2,4]triazolo[4,3-c]quinazolines **5a-5n** have been examined for cytotoxicity activity towards the breast cancer cell lines MCF-7 and MDA-MB231utilizing the MTT assay. The obtained results have been summarized in Table 1 in comparison to Camptothecin (Cmp) as a reference. Among all the screened compounds **5a-5n**, two of our quinazoline-triazoles molecule, 5-phenyl-3-(2,3,4-trimethoxyphenyl)-[1,2,4]triazolo[4,3-c]quinazoline **(5g)** and 3-(2,3-dichlorophenyl)-5-phenyl-[1,2,4]triazolo[4,3-c]quinazoline**(5j)** displayed better and comparable cytotoxic potential towards MCF-7 cell line exhibiting IC_{50} value of 1.14 mM and 1.39 mM, respectively (Table 2). Compound **5j** also displayed IC_{50} = 1.95 mM against MDA-MB231 cell line. Except, compound 3-(4-methylphenyl)-5-phenyl-[1,2,4]triazolo [4,3-c]quinazoline **(5c)** showing least antiproliferative efficacy with IC_{50} = 43.33 mM, all other synthesized quinazoline fused 1,2,4-triazole analogs displayed significant cytotoxicity. Here, dichloro- and trimethoxy-substituted [1,2,4]triazolo[4,3-c]quinazolines displayed improved potential in contrast to bis([1,2,4]triazolo)[4,3-a:4',3'-c]quinazolines as per our recent publication[47].

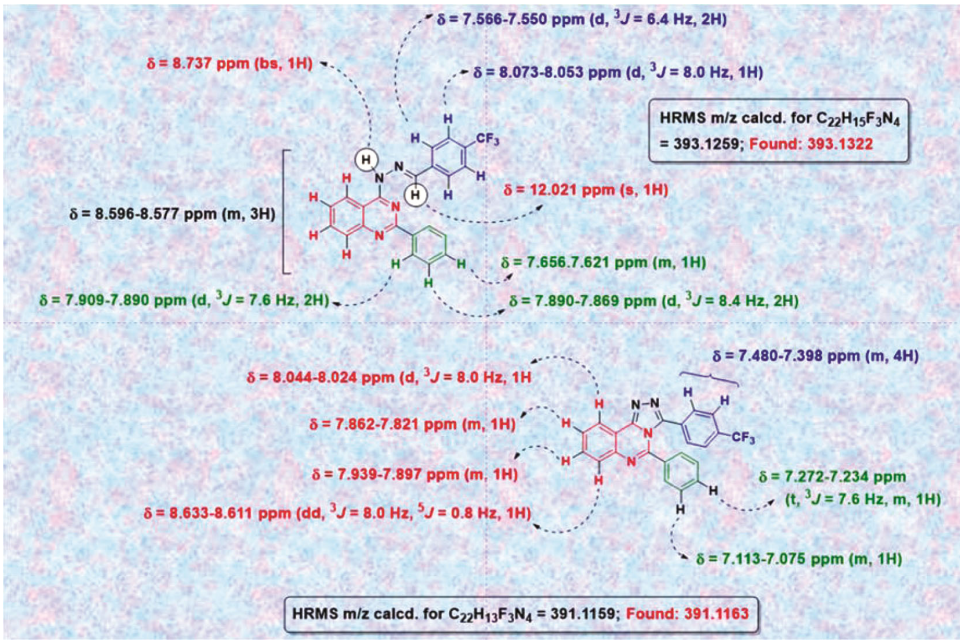

Fig. 2 — Spectral explanation for 5-phenyl-3-(4-(trifluoromethyl)phenyl) [1,2,4]triazolo[4,3-c]quinazoline **5l** and corresponding hydrazone **4l**.

Table 1 — Physical properties of 3-aryl-5-phenyl-[1,2,4]triazolo[4,3-c]quinazolines **5a-n**

Compd	M.Pt (°C)	R_f[a]	Yield (%)	Colour	Compd	M.Pt (°C)	R_f	Yield (%)	Colour
5a	162-164	0.23	55	Musturd	**5h**	208-210	0.41	68	White
5b	189-191	0.23	54	Brown	**5i**	216-218	0.22	75	White
5c	140-142	0.28	58	Off White	**5j**	188-190	0.23	76	White
5d	164-166	0.16	77	Orange	**5k**	124-126	0.28	80	White
5e	220-222	0.38	56	Brown	**5l**	238-240	0.62	81	White
5f	228-230	0.34	60	White	**5m**	250-252	0.81	86	White
5g	178-180	0.33	82	White	**5n**	260-262	0.63	80	White

Table 2 — Cytotoxicity of 3-aryl-5-phenyl-[1,2,4]triazolo[4,3-c]quinazolines **5a-n**against breast cancer cell lines (MCF-7& MDA-MB231).

Compd	R	IC_{50} (mM) (MCF-7)	IC_{50} (mM)MDA-MB231	Compd	R	IC_{50} (mM) (MCF-7)	IC_{50} (mM)MDA-MB231
5a	2-CH_3	1.84	–	**5h**	4-F	1.66	–
5b	3-CH_3	2.45	–	**5i**	4-Cl	1.81	2.11
5c	4-CH_3	43.33	–	**5j**	2,3-Cl	1.39	1.95
5d	4-$CH(CH_3)_2$	1.63	–	**5k**	Naphthyl	2.22	3.42
5e	4-OH	1.95	–	**5l**	4-CF_3	2.25	–
5f	4-OCH_3	nt*	–	**5m**	3-NO_2	4.08	2.44
5g	2,3,4-OCH_3	1.14	2.79	**5n**	4-NO_2	3.26	2.53
CPT	–	1.39	1.98	–	–	1.39	1.98

*nt: - not tested (–); CPT:- Camptothecin

Molecular Docking Studies

The site-specific molecular interaction was simulated using computer modelling to confirm the preceding conclusion. The compounds **5a**, **5d**, **5e**, **5g**, **5h**, **5i**, and **5j** were docked with **3u6j** using default docking protocol of Molecular Operating Environment (MOE). As the primary cause of cancer-related mortality for women worldwide, breast cancer is one of the most prevalent cancers[52].The poor prognosis associated with breast cancer is mostly caused by metastasis, a process in which tumor angiogenesis is essential. Tumor angiogenesis is mostly dependent on the activity of vascular endothelial growth factor receptor 2, or VEGFR-2, a cell membrane-bound tyrosine kinase receptor that was first discovered in endothelial cells[53-55]. Due to their significant importance, our docking methodology has selected these proteins as target receptors. Our goal was to determine the binding behavior in this case using the docking scores of synthesized compounds.This docking approach looked for binding sites on the protein's whole surface. The conformer with the lowest binding energy was sought for docking simulation, and the one with the lowest energy was acquired for further study.

The docking results, as shown in Fig. 3, suggested a robust binding of each compound to site 1 (where the ligand was crystalized in **3u6j** better than other sites. Further investigation revealed that the ligands interact with **3u6j** of the hydrophobic cave of **3u6j**'s site 1.

The compound **5a** is surrounded by residues such as Ile1044, Leu889, Val899, Ile888, Ile892, Leu1019, Ile1025, Arg1027, Glu885, Cys1024, His1026, Lys868, Asp1046, Cys1045, and Thr916 within proximity of 4.5 Å with binding energy of –6.14 $kcalmol^{-1}$. **5d** is surrounded by residues such as His1026, Gly1048, Arg1027, Ser884, Glu885, Ala881, Leu889, Ile1025, Ile888, Leu1019, Ile1044, Ile892, and Val898 within proximity of 4.5 Å with binding energy of –6.65 $kcalmol^{-1}$. **5e** is surrounded by residues such as Ile892, Ile1044, Val899, Leu1019, Ile1025, Val898, Thr916, Cys1045, Arg1027, His1026, Asp1046, Glu885, and Lys868 within proximity of 4.5 Å with binding energy of –6.49 $kcalmol^{-1}$. **5g** is surrounded by residues such as Ile1044, Val899, Ile892, Leu1019, Ile1025, Ile888, Val898, Leu889, Cys1024, Cys1045,Thr916, Lys868, Glu885, Asp1046, His1026, Arg1027 within proximity of 4.5 Å with a binding energy of –7.08 $kcalmol^{-1}$. **5h** is surrounded by residues such as His1026, Asp1046, Arg1027, Cys1045, Gly1048, Glu885, Leu1019, Ile1044, Val898, Ile892, Leu889, Ile1025, and Ile888 within proximity of 4.5 Å with binding energy of -6.39 $kcalmol^{-1}$.The compound **5i** is surrounded by residues such as Ile1025, Leu1019,

Ile1044, Val899, Ile892, Arg1027, His1026, Asp1046, Cys1045, Thr916, Glu885, Leu889, Lys868, Ile888, and Val898 which are in proximity of 4.5 Å (Fig. 2 and Table 3) and the **5i**-3u6j complex free energies of –6.34 kcalmol^{-1}. It demonstrates that the binds were mostly hydrophobic in nature. Further, **5i** shows NH(Arg1027)···Cl**(5i)**, NH(Asp1046)···π**(5i)**, and NH(Thr916)···π**(5i)** hydrogen bonding with

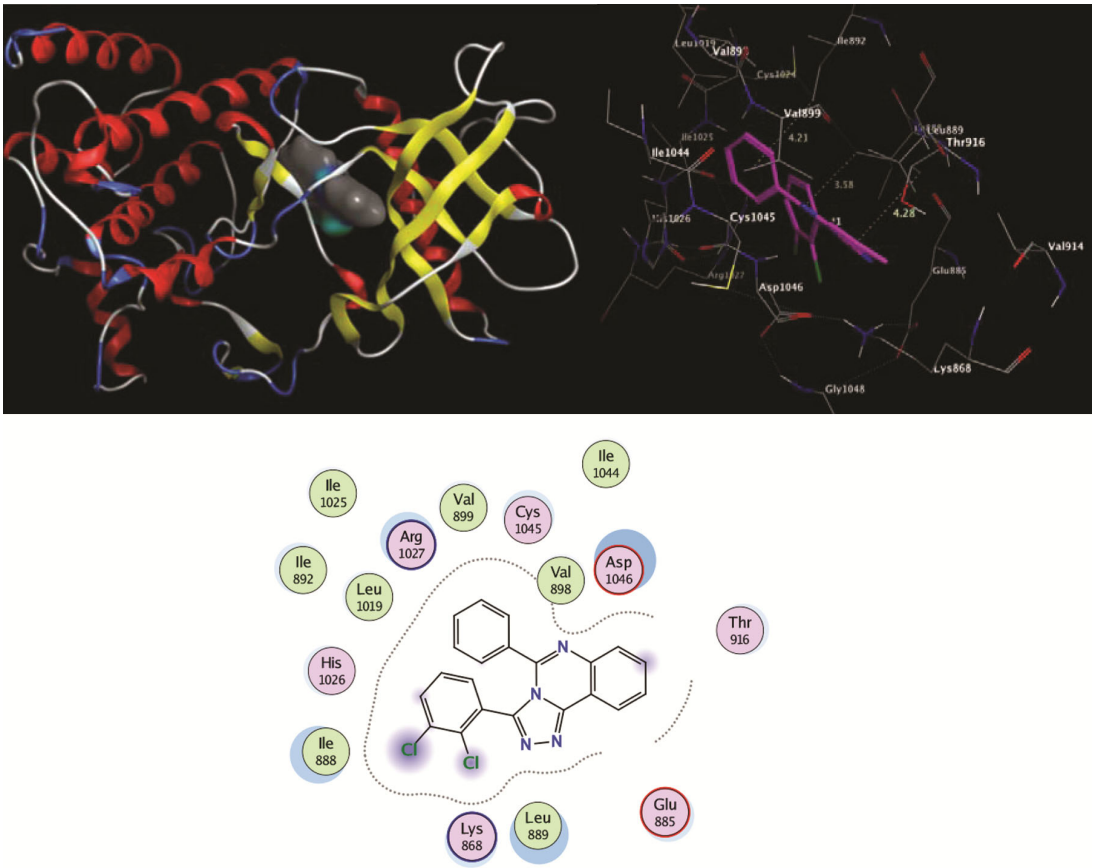

Fig. 3 — 2D representation of the binding interactions between the binding pose of **5j** and the active site of **3u6j**

Table 3 — Summary of surrounding residues and interaction of compounds with**3u6j**.

Compd	Binding energy kcalmol^{-1}	Surrounding residues in the proximity of 4.5Å	Hydrogen bonding interaction
5a	–6.15	Ile1044, Leu889, Val899, Ile888, Ile892, Leu1019, Ile1025, Arg1027, Glu885, Cys1024, His1026, Lys868, Asp1046, Cys1045, and Thr916	NH(ASP 1046)···π(5g) [3.34 Å]
5d	–6.65	His1026, Gly1048, Arg1027, Ser884, Glu885, Ala881, Leu889, Ile1025, Ile888, Leu1019, Ile1044, Ile892, and Val898	Hydrophobic interaction
5e	–6.49	Ile892, Ile1044, Val899, Leu1019, Ile1025, Val898, Thr916, Cys1045, Arg1027, His1026, Asp1046, Glu885, and Lys868	Hydrophobic interaction
5g	–7.08	Ile1044, Val899, Ile892, Leu1019, Ile1025, Ile888, Val898, Leu889, Cys1024, Cys1045, Thr916, Lys868, Glu885, Asp1046, His1026, Arg1027	Hydrophobic interaction
5h	–6.39	His1026, Asp1046, Arg1027, Cys1045, Gly1048, Glu885,Leu1019, Ile1044, Val898, Ile892, Leu889, Ile1025, and Ile888	Hydrophobic interaction
5i	–6.34	Ile1025, Leu1019, Ile1044, Val899, Ile892, Arg1027, His1026, Asp1046, Cys1045, Thr916, Glu885, Leu889, Lys868, Ile888, and Val898	NH(Arg1027)···Cl(5c) [2.31 Å], NH(Asp1046)···π(5c) [3.29 Å], NH(Thr916)···π(5c) [4.13 Å],
5j	–6.41	Ile1025, Val899, Ile1044, Ile892, Leu1019, Ile888, Leu889, Arg1027, Cys1045, Asp1046, His1026, Lys868, and Glu885, Thr916	CH(Ile892)···π(5d) [4.21 Å], CH(Ile888)···π(5d) [3.58 Å], CH(Thr916)···π(5d) [4.28 Å],

interacting distance of 2.31 Å, 3.29 Å, and 4.13 Å, respectively. Similarly, **5j** is surrounded by residues (Fig. 4) such as Ile1025, Val899, Ile1044, Ile892, Leu1019, Ile888, Leu889, Arg1029, Cys1045, Asp1046, His1026, Lys868, and Glu885 within proximity of 4.5 Å with bindingenergy of –6.41 kcalmol^{-1}. Therefore, these results showed that interactions facile the kinase inhibition activity of synthesized compounds.

Antioxidant Studies

Considering the admirable antioxidant efficacy of some 1,2,4-triazolo[1,5-a]quinazolines[56, 57], the newly prepared 3-aryl-5-phenyl-[1,2,4]triazolo[4,3-c]quinazolines **5a-5n** also have been assessed for antioxidant activity (ABTS Radical Scavenging Assay) and 50% inhibitory concentration have been presented in Table 4. Compound **5h** with *para*-fluorine substituent displayed

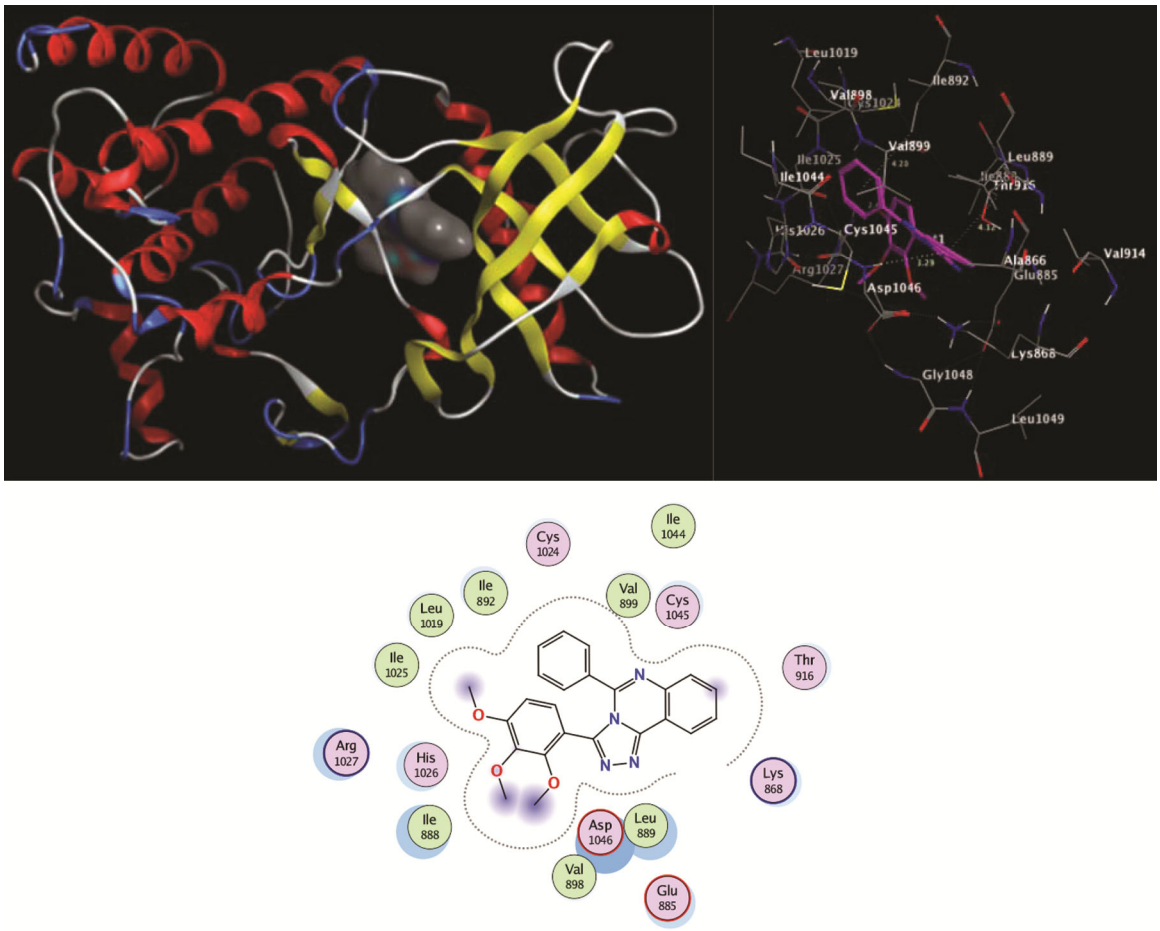

Fig. 4 — 2D representation of the binding interactions between the binding pose of **5g** and the active site of **3u6j**

Table 4 — ABTS Radical scavenging abilityof 3-aryl-5-phenyl-[1,2,4]triazolo[4,3-c]quinazolines **5a-n**

Compd	R	IC_{50} value (µg/mL) (Mean ± SEM)	Compd	R	IC_{50} value (µg/mL) (Mean ± SEM)
5a	2-CH_3	185.5 ± 0.14	**5h**	4-F	11.2 ± 0.14
5b	3-CH_3	181.3 ± 0.095	**5i**	4-Cl	108.3 ± 0.17
5c	4-CH_3	288.1 ± 0.08	**5j**	2,3-Cl	128.1 ± 0.17
5d	4-$CH(CH_3)_2$	ADL	**5k**	Naphthyl	76.18 ± 0.27
5e	4-OH	76.89 ± 0.08	**5l**	4-CF_3	ADL
5f	4-OCH_3	300.1 ± 0.06	**5m**	3-NO_2	ADL
5g	2,3,4-OCH_3	65.59 ± 0.1	**5n**	4-NO_2	163.1 ± 0.11
AsA	–	5.191 ± 0.03	**–**	–	–

*ADL: Above dose limit (above 1000 µg/mL); AsA - Ascorbic Acid

highest antioxidant activity with IC_{50} value of 11.2 ± 0.14 µg/mL. This means 11.2 µg of **5h** was found equivalent to 5.19 µg of ascorbic acid (standard). Compounds **5e**, **5g**, and **5k** also shows significant scavenging potential, showing IC_{50} in the range of 65.59 ± 0.1 to 76.89 ± 0.08 µg/mL. From Table 4, we can demonstrate that, the declining order of their radical scavenging capacity as **5h>5g>5k>5e>5i>5j>5n>5b>5a>5c>5f**. Other remaining three compounds **5d**, **5l** and **5m** exhibited extremely poor antioxidant activity (above1000 µg/mL). The percentage inhibition results of each compound at different concentration has been presented in Fig. 5.

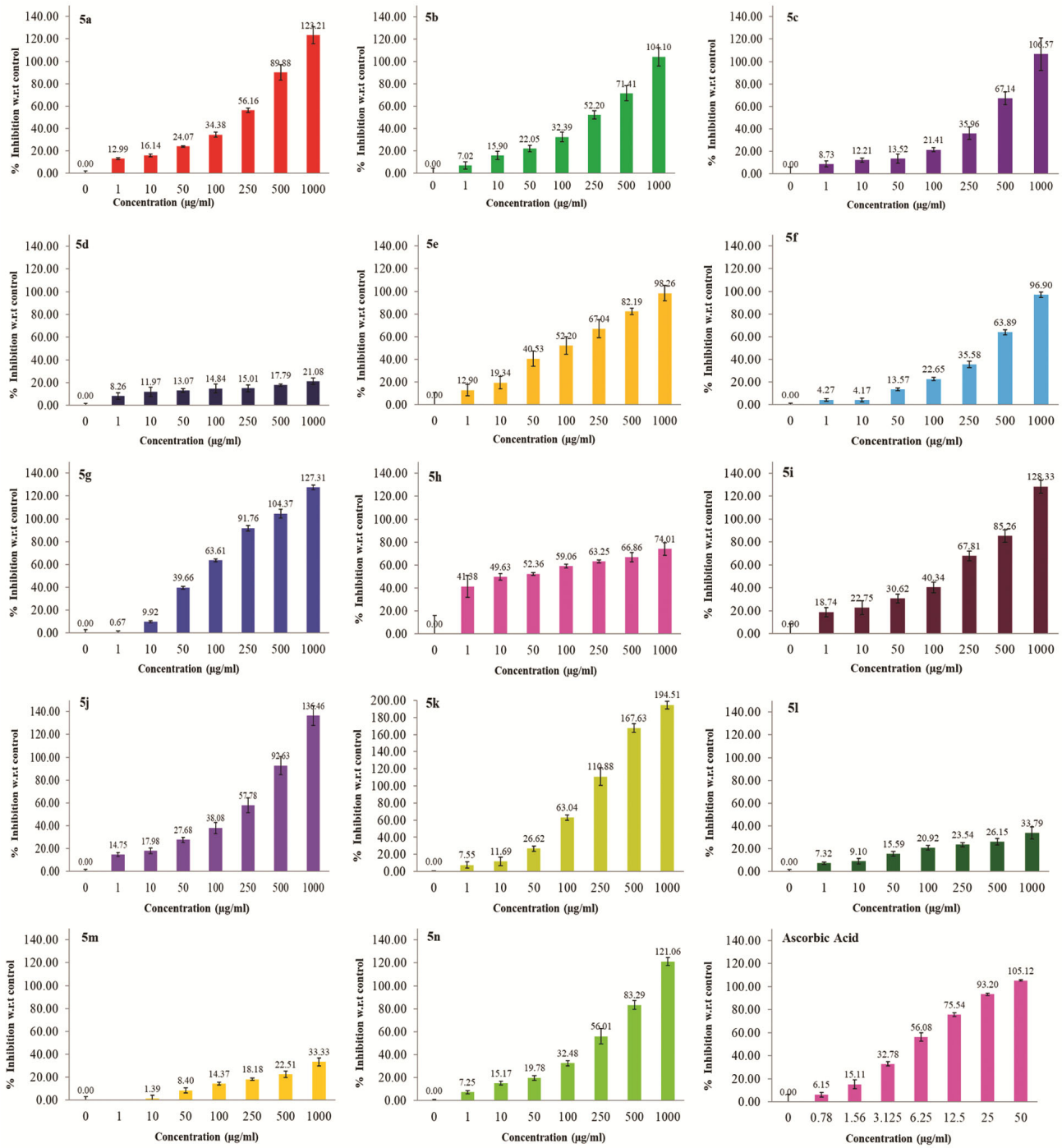

Fig. 5 — ABTS radical scavenging ability of 3-aryl-5-phenyl-[1,2,4]triazolo[4,3-c]quinazolines **5a-5n**at different concentrations.

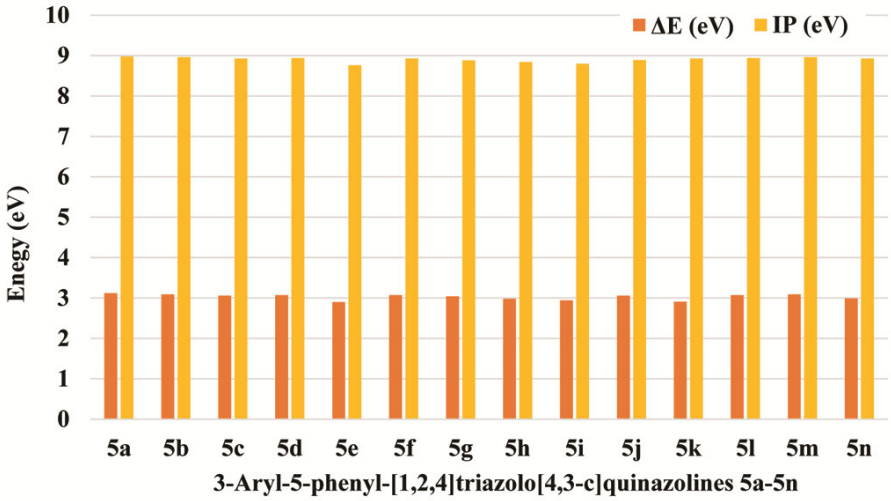

Fig. 6 — Energy gap and ionization potential profile of 3-aryl-5-phenyl-[1,2,4]triazolo[4,3-c]quinazolines**5a-5n**.

DFT Studies

Synthesized compounds were optimized at ground state (S_0) using density functional theory (DFT) at the B3LYP/6-311G(d) level using Gaussian 16[58, 59]. The absence of imaginary vibration frequencies analyzed the stability of molecular structures. The electronic properties of compounds such as the ionization energy (I), electron affinity (A), electronegativity (χ), chemical potential (μ), absolute hardness (η), global softness (σ), and electrophilicity index (ω), were determined using the band gap energy (Egap = E_{HOMO} − E_{LUMO}) and the HOMO/LUMO energies. Frontier molecular orbitals are used to determine these properties as main orbitals involved in chemical stability. A molecule's reactivity can be explained by considering its chemical hardness, which is directly related to the HOMO−LUMO energy gap. A molecule with a greater E_{gap} or chemical hardness is less reactive[60-62]. All of these parameters are crucial for calculating the stability and reactivity of molecules. One of the key quantum chemical parameters that characterize the toxicity of many pollutants in terms of their site selectivity and reactivity is the electrophilicity index, or ω. Additionally, the biological potency of drug-receptor interaction is calculated by electrophilicity.

Additionally, the energy gap between frontier molecular orbitals and the ionization potential (IP) were used to assess antioxidant properties. First, we used Koopman's theory to predict these compounds' antioxidant activities[63].

$IP = -E_{HOMO}$

The compound's ability to donate electrons is enhanced by a smaller IP, which in turn results in a higher antioxidant capacity. The obtained IP values of these compounds are shown in Fig. 6, and they are in the following order: **5a>5m>5b>5l>5d>5n>5k>5c>5f>5j>5g>5h>5i>5e**. This suggests that these compounds' antioxidant activities gradually increase as the substation of electron-donating groups increases.

Furthermore, as per earlier research[64-66], the energy gap (ΔE) is a crucial parameter to determine the compound's antioxidant activity, with a smaller energy gap potentially increasing the antioxidant activity. The order of these compounds' calculated energy gaps, which are displayed in Fig. 6 is **5a>5m>5b>5l>5d>5f>5j>5c>5g>5n>5h>5i>5k>5e**. This suggests that the compounds' antioxidant activities would improve in almost same order (with slight deviation) as the amount of electron-donating substitution increases (Table 5). The HOMO-LUMO plots of the compounds are given in Table 6.

Structure Activity Relationship (SAR)

It was identified that the presence of additional chlorine substituents on the aryl ring significantly decreases IC_{50} from 1.81mM to 139 mM. Similarly, presence of additional $-OCH_3$ group boost radical scavenging ability by reducing IC_{50} value to 65.59 ± 0.1μg/mL **(5f)** from 300.1 ± 0.06 μg/mL **(5g)**. However, as the number of halogens increases, required IC_{50} value increase from 108.3 ± 0.17 μg/mL **(5i)** to 128.1 ± 0.17 μg/mL **(5j)** and above dose limit (100 μg/mL) **(5l).**

Table 5 — Electronic properties of 3-aryl-5-phenyl-[1,2,4]triazolo[4,3-c]quinazolines **5a-n**

Compd	HOMO (H; eV)	LUMO (L; eV)	E gap (ΔE; eV)	Ionization Potential (I, eV)	Electron affinity (A)	Electronegativity (X; eV)	Chemical Potential (μ; eV)	Chemical hardness (η; eV)	Chemical Softness (σ)	Electrophilicity index (ω)
5a	–8.98	–5.86	3.12	8.98	5.86	7.42	–7.42	1.56	0.32	17.65
5b	–8.96	–5.87	3.09	8.96	5.87	7.42	–7.42	1.55	0.32	17.76
5c	–8.93	–5.87	3.06	8.93	5.87	7.4	–7.4	1.53	0.33	17.9
5d	–8.94	–5.87	3.07	8.94	5.87	7.41	–7.41	1.54	0.32	17.83
5e	–8.76	–5.86	2.9	8.76	5.86	7.31	–7.31	1.45	0.34	18.43
5f	–8.93	–5.86	3.07	8.93	5.86	7.4	–7.4	1.54	0.32	17.78
5g	–8.88	–5.84	3.04	8.88	5.84	7.36	–7.36	1.52	0.33	17.82
5h	–8.84	–5.86	2.98	8.84	5.86	7.35	–7.35	1.49	0.34	18.13
5i	–8.8	–5.86	2.94	8.8	5.86	7.33	–7.33	1.47	0.34	18.28
5j	–8.89	–5.83	3.06	8.89	5.83	7.36	–7.36	1.53	0.33	17.7
5k	–8.93	–6.02	2.91	8.93	6.02	7.48	–7.48	1.46	0.34	19.16
5l	–8.94	–5.87	3.07	8.94	5.87	7.41	–7.41	1.54	0.32	17.83
5m	–8.96	–5.87	3.09	8.96	5.87	7.42	–7.42	1.55	0.32	17.76
5n	–8.93	–5.94	2.99	8.93	5.94	7.44	–7.44	1.5	0.33	18.45

Table 6 — HOMO-LUMO representation of 3-aryl-5-phenyl-[1,2,4]triazolo[4,3-c]quinazolines **5a-n**

Compd	Optimized structure	HOMO	LUMO
5a	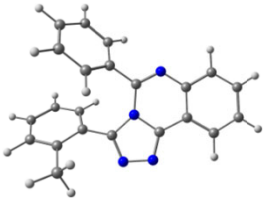	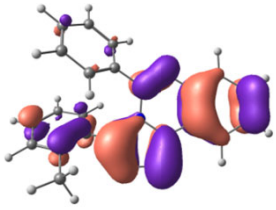	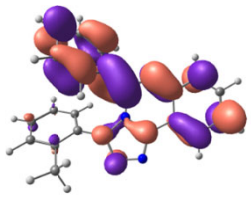
5b	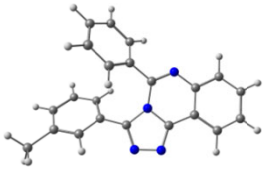	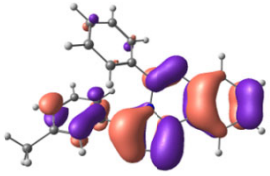	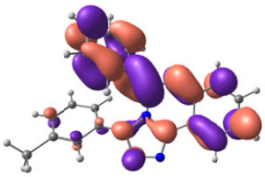
5c	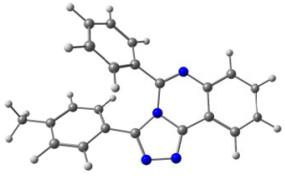	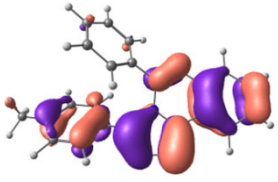	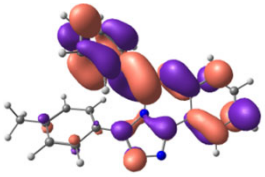
5d	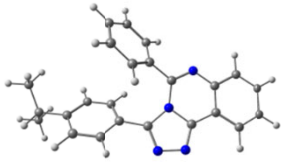	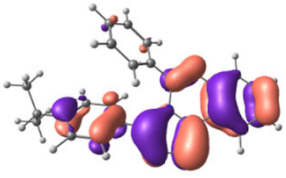	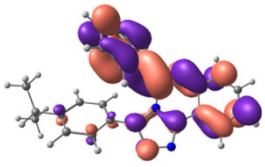

(*Contd.*)

Table 6 — HOMO-LUMO representation of 3-aryl-5-phenyl-[1,2,4]triazolo[4,3-c]quinazolines **5a-n** (*Contd.*)

Compd	Optimized structure	HOMO	LUMO
5e	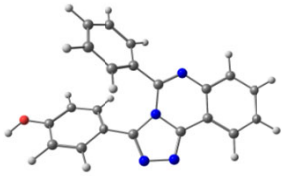	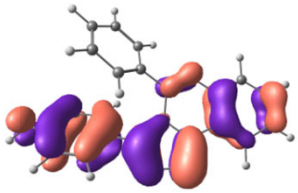	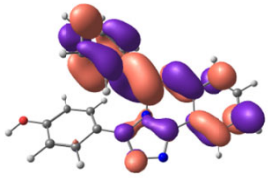
5f	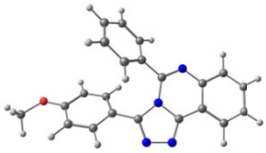	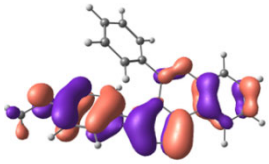	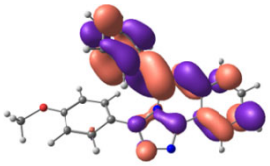
5g	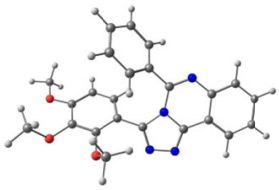	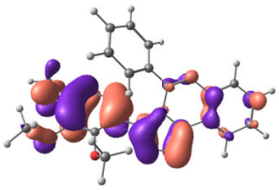	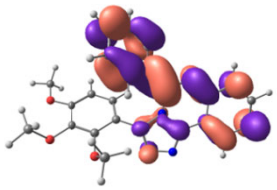
5h	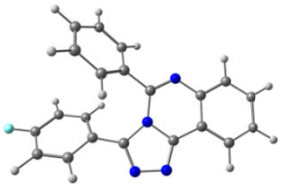	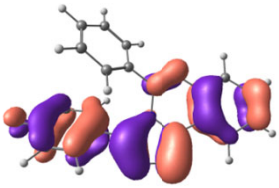	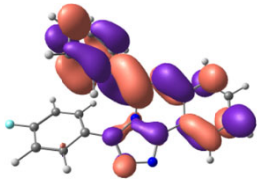
5i	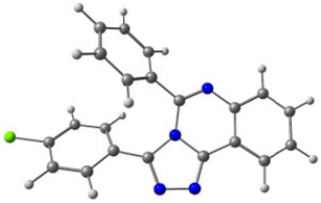	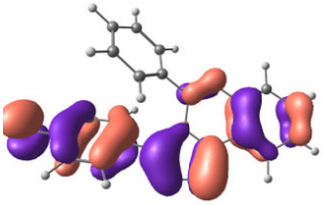	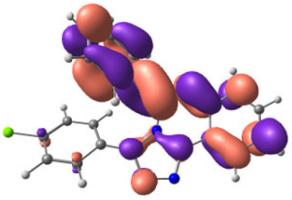
5j	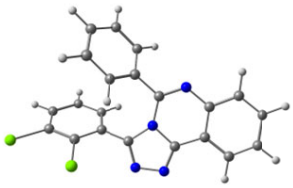	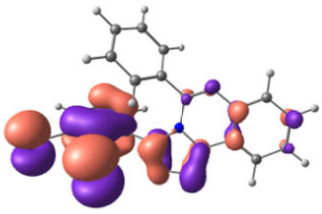	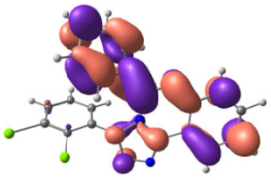
5k	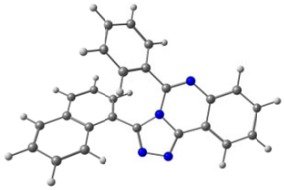	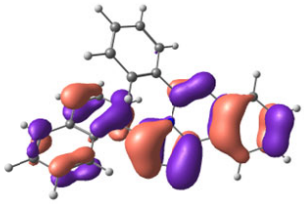	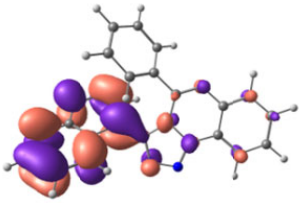
5l	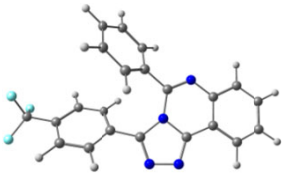	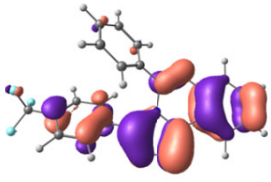	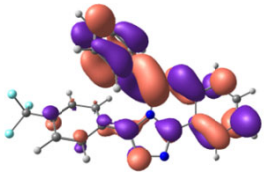

(*Contd.*)

Table 6 — HOMO-LUMO representation of 3-aryl-5-phenyl-[1,2,4]triazolo[4,3-c]quinazolines **5a-n** (*Contd.*)

Compd	Optimized structure	HOMO	LUMO
5m	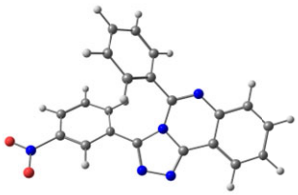	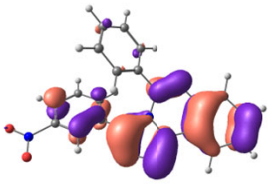	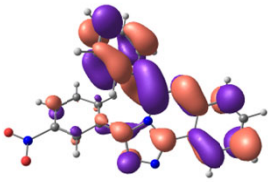
5n	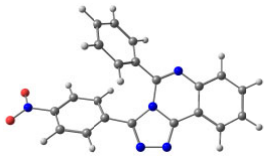	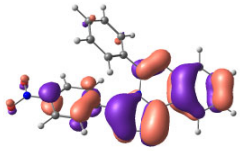	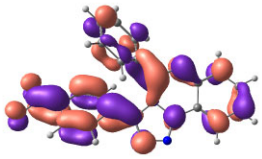

Conclusions

In conclusion, synthesis, antiproliferative, and antioxidant studies of twelve newly synthesized 3-aryl-5-phenyl-[1,2,4]triazolo[4,3-c]quinazolines **5a-5n** have been conducted. New (*E*)-4-(2-benzylidenehydrazineyl)-2-phenylquinazolines **4a-4n** was subjected as a key precursor under cyclization to afford **5a-5n**. Antiproliferative activity examination led to the identification of 5-phenyl-3-(2,3,4-trimethoxyphenyl)-[1,2,4]triazolo[4,3-c]quinazoline **(5g)**, as most active, which exhibits optimal cytotoxicity with an IC_{50} value of 1.14 mM against MCF-7 cancer cell line, but significantly compared to standard. Additionally, molecular modelling studies have been conducted to support the results and to study the binding interaction of the compound **5g** and **5j** into VEGFR-2 kinase enzyme. Furthermore, compound **5h** demonstrated uppermost antioxidant activity (IC_{50}= 11.2 ± 0.14 µg/mL).

Acknowledgements

Dr. Ravinder Kumar and Parul Kaushik acknowledge the support received from the Department of Chemistry, Maharishi Markandeshwar (Deemed to be University), Mullana, Ambala, Haryana (INDIA) for providing an opportunity to carry out research studies, infrastructure, and financial facilities. The authors are also grateful to Akaar Biotech Pvt. Ltd., Lucknow, Uttar Pradesh (India) for antioxidant activities. The authors are also extremely indebted to all the researchers identified in the references, who carried out this thought-provoking work on triazoloquinazoline.

Supplementary Information

Supplementary information is available in the website http://nopr.niscpr.res.in/handle/123456789/ 58776.

References

1 Siegel R L, Miller K D, Wagle N S & Jemal A, *Ca Cancer J Clin,* 73 (2023) 17.
2 Niu N, Ma S, Zhang L, Liu Q & Zhang S, *Molecules,* 27 (2022) 3906.
3 Ahmad I, *Med Chem Comm,* 8 (2017) 871.
4 Bansal R & Malhotra A, *Eur J Med Chem,* 211 (2021) 113016.
5 Boddapati S M, Bollikolla H B, Saini, H S, Ramesh N & Jonnalagadda S B, *Arab J Chem,* 16 (2023) 105190.
6 Bouchut A, Rotili D, Pierrot C, Valente S, Lafitte S, Schultz J, Hoglund U, Mazzone R, Lucidi A & Fabrizi G, *Eur J Med Chem,* 161 (2019) 277.
7 Li Z, Zhao L, Bian Y, Li Y, Qu J & Song F, *Curr Top Med Chem,* 22 (2022) 1035.
8 Wang Y, Song H, Wang S, Cai Q, Zhang Y, Zou Y, Liu X & Chen J, *Pestic Biochem Phys,* 189 (2023) 105310.
9 Haider K, Das S, Joseph A & Yar M S, *Drug Dev Res,* 83 (2022) 859.
10 Das R, Mehta D K & Dhanawat M, *Anti-Cancer Agent Med Chem,* 21 (2021) 1350.
11 Moradi M, Mousavi A, Emamgholipour Z, Giovannini J, Moghimi S, Peytam F, Honarmand A, Bach S & Foroumadi A, *Eur J Med Chem,* 259 (2023) 115626.
12 Haghighijoo Z, Zamani L, Moosavi F & Emami S, *Eur J Med Chem,* 227 (2022) 113949.
13 Zayed M F, *Chem Eng, 6* (2022) 94.
14 Dutta A & Sarma D, *Tuberculosis,* 124 (2020) 101986.
15 Buchler A, Ismailani U S, MacMullin N, Abdirahman F, Adi M, Bi C, Jany C, Keillor J W & Rotstein B H, *J Med Chem.,* 66 (2023) 6682.
16 Auti P S, George G & Paul A T, *RSC Adv*,10 (2020) 41353.
17 Bhatia P, Sharma V, Alam O, Manaithiya A, Alam P, Alam M T & Imran M, *Eur J Med Chem*, 204 (2020) 112640.
18 Abdelli A, Azzouni S, Plais R, Gaucher A, Efrit M L & Prim D, *Tetrahedron Lett,* 86 (2021) 153518.
19 Sathyanarayana R & Poojary B, *J Chin Chem Soc,* 67 (2020) 459.
20 Kazeminejad Z, Marzi M, Shiroudi A, Kouhpayeh S A, Farjam M & Zarenezhad E, *Biomed Res Int,* (2022) 2022.
21 Strzelecka M & Świątek P, *Pharm*, 14 (2021) 224.
22 Boraei A T, Singh P K, Sechi M & Satta S, *Eur J Med Chem*, 182 (2019) 111621.
23 Grytsai O, Valiashko O, Penco-Campillo M, Dufies M, Hagege A, Demange L, Martial S, Pagès G, Ronco C & Benhida R, *Bioorg Chem*, 104 (2020) 104271.

24 Leenders R G, Brinch S A, Sowa S T, Amundsen-Isaksen E, Galera-Prat A, Murthy S, Aertssen S, Smits J N, Nieczypor P & Damen E, *J Med Chem*, 64 (2021) 17936.
25 Paprocka R, Kołodziej P, Wiese-Szadkowska M, Helmin-Basa A & Bogucka-Kocka A, *Molecules*, 27 (2022) 4488.
26 Abuelizz H A & Al-Salahi R, *Bioorg Chem*, 115 (2021) 105263.
27 Zeydi M M, Montazeri N & Fouladi M, *J Heterocycl Chem,* 54 (2017) 3549.
28 Al-Salahi R, El-Tahir K E, Alswaidan I, Lolak N, Hamidaddin M & Marzouk M, *Chem Cent J,* 8 (2014) 1.
29 Alagarsamy V & Pathak U S, *Bioorg Med Chem,* 15 (2007) 3457.
30 Zhang C B, Yang C W, Deng X Q & Quan Z S, *Med Chem Res*, 21 (2012) 3294.
31 Zhang H J, Jin P, Wang S B, Li F N, Guan L P, Quan Z S, *Arch Pharm*, 348 (2015) 564.
32 Danylchenko S Y, Kovalenko S, Drushlyak O, Kovalenko S & Maes L *Ukr Biopharm J*, 42 (2016) 78.
33 Almehizia A A, Abuelizz H A, Taie H A, ElHassane A, Marzouk M & Al-Salahi R, *Saudi Pharm J*, 27 (2019) 133.
34 Abuelizz H A, Anouar E H, Ahmad R, Azman N I I N, Marzouk M & Al-Salahi R, *PLoS One*, 14 (2019) e0220379.
35 El-Adl K, Ibrahim M K, Alesawy M S & Eissa I H, *Arch Pharm*, 355 (2022) 2100506.
36 Al-Salahi R A, Al-Omar M A, Alswaidan I, Marzouk M, El-Senousy W M & Amr A E G E, *Res Chem Intermed*, 41 (2015) 151.
37 Antypenko L M, Kovalenko S I, Los' T S & Rebec' O L, *J Heterocycl Chem*, 54 (2017) 1267.
38 Patel D M, Vala, R M, Sharma M G, Rajani D P & Patel H M, *Chem Sel*, 4 (2019) 1031.
39 Gineinah M M, Nasr M, Abdelal A, El-Emam A & Said S, *Med Chem Res,* 10 (2000) 243.
40 Mohamed M, Ibrahim M, Alafify A, Abdel-Hamide S & Mostafa A, *Int J Pharm,* 1 (2005) 261.
41 El-Shershaby M H, Ghiaty A, Bayoumi A H, Al-Karmalawy A A, Husseiny E M, El-Zoghbi M S & Abulkhair H S, *Bioorg Med Chem*,42(2021) 116266.
42 Antypenko O M, Kovalenko S I, Karpenko O V, Nikitin V O & Antypenko L M, *Helv Chim Acta*, 99 (2016) 621.
43 Driowya M, Leclercq J, Verones V, Barczyk A, Lecoeur M, Renault N, Flouquet N, Ghinet A, Berthelot P & Lebegue N, *Eur J Med Chem,* 115 (2016) 393.
44 Al-Salahi R, Marzouk M, Ashour A & Alswaidan I, *Asian J Chem,* 26 (2014) 2173.
45 Ewes W A, Elmorsy M A, El-Messery S M & Nasr M N, *Bioorg Med Chem,* 28 (2020) 115373.
46 Alesawy M S, Al-Karmalawy A A, Elkaeed E B, Alswah M, Belal A, Taghour M S & Eissa I H, *Arch Pharm,* 354 (2021) 2000237.
47 Gheshlaghi S Z, Ebrahimi A, Faghih Z, Faghih Z, Shahraki A & Emami L, *Tetrahedron*,147 (2023) 133650.
48 Kumar R, Bains O, Kamal R, Kumar A, Kaur S, Bansal A & Chetti P, *Chem Sel,* 8 (2023) e202303876.
49 Kamal R, Kumar R, Kumar V, Kumar V, Bansal K K & Sharma P C, *Chem Sel,* 4 (2019) 713.
50 Kumar R, Kumar V, Kamal R, Kumar A, Kaur S, Bansal A & Chetti P, *Chem Sel,* 7 (2022) e202202635.
51 Kamal R, Kumar R, Kumar V, Bhardwaj J K, Saraf P, Kumar A, Pandit K, Kaur S, Chetti P & Beura S, *J Biomol Struct Dyn,* 39 (2021) 4398.
52 Liu Y, Ji R, Li J, Gu Q, Zhao X, Sun T, Wang J, Li J, Du Q & Sun B, *J Exp Clin Cancer Res*, 29 (2010) 1.
53 Millauer B, Wizigmann-Voos S, Schnürch H, Martinez R, Møller N, P H, Risau W & Ullrich A, *Cell*, 72 (1993) 835.
54 Hicklin D J & Ellis L M, *J Clin Oncol,* 23 (2005) 1011.
55 Guo S, Colbert L S, Fuller M, Zhang Y & Gonzalez-Perez R R, *BBA-Rev Cancer*, 1806 (2010) 108.
56 Al-Salahi R, Anouar E H, Marzouk M, Taie H A & Abuelizz H A, *Future Med Chem,* 10(2018) 379.
57 Sompalle R, Roopan S M, Al-Dhabi N A, Suthindhiran K, Sarkar G & Arasu M V, *J Photochem Photobiol B*, 162 (2016) 232.
58 Kumar A, Trivedi M, Sharma R K & Singh G, *New J Chem*, 41 (2017) 8459.
59 Frisch M E, Trucks G, Schlegel H, Scuseria G, Robb M, Cheeseman J, Scalmani G, Barone V, Petersson G & Nakatsuji H, *Gaussian 16, revision C. 01*, (Gaussian, Inc., Wallingford CT) 2016.
60 Muscat J, Wander A & Harrison N, *Chem Phys Lett*, 342 (2001) 397.
61 Rienstra-Kiracofe J C, Barden C J, Brown S T & Schaefer H F, *J Phys Chem A,* 105 (2001) 524.
62 Vektariene A, Vektaris G & Svoboda J A, *Arkivoc,* VII(2009) 311.
63 Leach A R, *Molecular modelling: principles and applications*, Pearson education 2001.
64 Joshi B D, Srivastava A, Honorato S B, Tandon, P O, Pessoa D L, Fechine P B A & Ayala A P, *Spectrochim Acta A Mol Biomol Spectrosc*, 113 (2013) 367.
65 Rajan V K, Hasna C & Muraleedharan K, *Food Chem*, 262 (2018) 184.
66 Rackova L, Firakova S, Kostalova D, Stefek M, Sturdik E & Majekova M, *Biorg. Med Chem*, 13 (2005) 6477.
67 Mickisch G, Fajta S, Keilhauer G, Schlick E, Tschada R & Alken P, *Urol Res*, 18 (1990) 131.
68 Cao G & Prior R L, *Clin Chem*, 44 (1998) 1309.
69 Kambayashi Y, Binh N T, Asakura H W, Hibino Y, Hitomi Y, Nakamura H & Ogino K, *J Clin Biochem Nutr*, 44 (2009) 46.
70 Gupta R, Sharma M, Lakshmy R, Prabhakaran D & Reddy K S, *Indian J Biochem Biophys*, 46 (2009) 126.